Biogeosciences
Discussions

Isotopic evidence for alteration of nitrous oxide emissions and producing pathways contribution under nitrifying conditions

Guillaume Humbert[1, 2, *], Mathieu Sébilo[1, 3], Justine Fiat[4], Longqi Lang[5], Ahlem Filali[4], Véronique Vaury[1], Mathieu Spérandio[5], Anniet M. Laverman[2]

5 [1]Sorbonne Université, CNRS, INRA, IRD, UPD, UPEC, Institute of Ecology and Environmental Sciences –Paris, iEES, F-75005 Paris, France
[2]Centre National de la Recherche Scientifique (CNRS), ECOBIO – UMR 6553, Université de Rennes, 35042 Rennes, France
[3]CNRS/Univ. Pau & Pays Adour/E2S UPPA, Institut des Sciences Analytiques et de Physico-Chimie pour l'Environnement et les Matériaux, UMR 5254, 64000, Pau, France
10 [4]Irstea, UR PROSE, CS 10030, F-92761, Antony Cedex, France
[5]LISBP, Université de Toulouse, CNRS, INRA, INSA, Toulouse, France

Correspondence to: Guillaume Humbert (g.humbert86@gmail.com)

Abstract. Nitrous oxide (N_2O) emissions by a nitrifying biofilm reactor were investigated with N_2O isotopocules. The site preference of N_2O (^{15}N-SP) indicated the contribution of producing and consuming pathways in response to changes in
15 oxygenation level (from 0 to 21 % O_2 in the gas mix), temperature (from 13.5 to 22.3 °C), and ammonium concentrations (from 6.2 to 62.1 mg N L^{-1}). Nitrite reduction, either nitrifier-denitrification or heterotrophic denitrification, was the main N_2O producing pathway under the tested conditions. Nitrite oxidation rates decreased as compared to ammonium oxidation rates at temperatures above 20 °C and sub-optimal oxygen levels, increasing N_2O production by the nitrite reduction pathway. Below 20 °C, a difference in temperature sensitivity between hydroxylamine and ammonium oxidation rates is most likely responsible
20 for an increase in the N_2O production via the hydroxylamine oxidation pathway (nitrification). A negative correlation between the reaction kinetics and the apparent isotope fractionation was additionally shown from the variations of $\delta^{15}N$ and $\delta^{18}O$ values of N_2O produced from ammonium.

1 Introduction

Nitrogen (N) cycling lies on numerous biological processes exploited and altered by anthropic activities (Bothe et al., 2007).
25 One of the major issues related to N cycle alteration is the production of nitrous oxide (N_2O) a potent ozone-depleting and greenhouse gas whose emissions exponentially increased during the industrial era (Crutzen et al., 1979; IPCC, 2014; Ravishankara et al., 2009). Wastewater resource recovery facilities (WRRFs) contribute to about 3 % of annual global anthropogenic N_2O sources (ca. 6.7 ± 1.3 Tg N-N_2O in 2011; IPCC, 2014); with 0 to 25 % of the influent nitrogen loads emitted as N_2O (Law et al., 2012b). The challenges in mitigation of these emissions rely on the understanding of the N_2O
30 producing processes and their controls.

1

Two microbial processes are responsible for the production of N$_2$O (nitrification and denitrification), with only one of these capable of consuming it (Kampschreur et al., 2009) (denitrification; Fig. 1a). Nitrification is the oxidation of ammonium to nitrite (NO$_2^-$) via the intermediate hydroxylamine (NH$_2$OH) conducted by ammonia oxidizers and the subsequent oxidation of NO$_2^-$ to nitrate (NO$_3^-$) by nitrite oxidizers. During nitrification, N$_2$O can be produced as reaction side-product from

35   hydroxylamine oxidation by biotic, abiotic or hybrid processes (Caranto et al., 2016; Heil et al., 2015; Terada et al., 2017). Heterotrophic denitrification and nitrifier-denitrification produce N$_2$O from nitrite reduction conducted by denitrifiers and ammonium oxidizers, respectively.

Temperature, electron donor and acceptor concentrations have been identified to control the N$_2$O emission from WRRFs (Bollon et al., 2016; Kampschreur et al., 2009; Tallec et al., 2006; Wunderlin et al., 2012). These variables may induce N$_2$O

40   accumulation due to inhibition or disturbance of enzyme activity (Betlach and Tiedje, 1981; Kim et al., 2008; Otte et al., 1996). In addition to this, the different N$_2$O producing processes, nitrification, nitrifier-denitrification or heterotrophic denitrification, are rarely observed independently from each other in heterogeneous environments like wastewater. However, the understanding of the influence that environmental conditions have on the balance between these processes and the N$_2$O producing pathways remain to a large extend unexplored.

45   In order to decipher N$_2$O producing/consuming pathways, the analysis of N$_2$O isotopocules, molecules that only differ in either the number or position of isotopic substitutions, has been applied (Koba et al., 2009; Sutka et al., 2006) (Figs. 1b-d). The isotope composition of substrates and fractionation mechanisms influence both nitrogen and oxygen isotope ratios of N$_2$O (reported as δ^{15}N and δ^{18}O, respectively, Fig. 1b). Basically, the oxygen atom in the N$_2$O molecule produced by hydroxylamine oxidation originates from atmospheric dissolved oxygen with δ^{18}O of 23.5 ‰ (Andersson and Hooper, 1983; Hollocher et al.,

50   1981; Kroopnick and Craig, 1972), while the oxygen atom in N$_2$O produced by nitrite reduction originates from nitrite that has undergone oxygen-exchange with water (Kool et al., 2007; Snider et al., 2012). Nonetheless, the δ^{18}O-N$_2$O resulting from the nitrite reduction conducted by the nitrifiers ranges from 13 to 35 ‰ (Snider et al., 2012). In contrast, the N$_2$O produced by the denitrifiers through the nitrite reduction pathway has δ^{18}O over 35 ‰ (Snider et al., 2013). However, the O-exchange between the N$_2$O precursors and water can decrease it to values below 35 ‰ (Snider et al., 2015). Therefore, the δ^{18}O alone

55   does not enable differentiation between the N$_2$O producing pathways.

In combination with δ^{18}O, the δ^{15}N-N$_2$O allows to identify the N$_2$O producing pathways (Fig. 1b). However, the isotope fractionations (or isotope effects) largely influence the δ^{15}N-N$_2$O due to wide variations between and within the reactions involved in the nitrogen cycle (Denk et al., 2017). The isotopic fractionations result from the difference in equilibrium constant (abiotic process) or reaction rate (biotic process) observed between the heavier and lighter isotopes. The net isotope effects (Δ)

60   approximated from the difference between δ^{15}N of product and substrate characterize the production of compounds resulting from sequential or branched reactions and have been recently reviewed (Denk et al., 2017; Toyoda et al., 2017). So far, only two estimates of the net isotope effect of N$_2$O production by ammonium oxidation via hydroxylamine of -46.9 and -32.6 ‰ have been proposed (Sutka et al., 2006; Yamazaki et al., 2014). These values are imbricated between -52.8 and -6 ‰, the range

Biogeosciences
Discussions

of net isotope effects related to the N_2O production through nitrite reduction performed by nitrifiers or denitrifiers (Lewicka-Szczebak et al., 2014; Sutka et al., 2008).

Similarly to isotope ratios, the nitrogen isotopomer site preference (^{15}N-SP), the difference between the relative abundances of N_2O molecules enriched in the central (N^α) position and in the terminal (N^β) position, differ according to N_2O producing pathway (Figs. 1c and d). During heterotrophic or nitrifier-denitrification the ^{15}N-SP of N_2O produced from nitrate or nitrite ranges from -10.7 to 0.1 ‰, while ranging from 13.1 to 36.6 ‰ when N_2O results from hydroxylamine oxidation (Frame and Casciotti, 2010; Jung et al., 2014; Sutka et al., 2006; Yamazaki et al., 2014). Finally, N_2O reduction to N_2 by heterotrophic denitrifiers increases the values of δ^{15}N, δ^{18}O and ^{15}N-SP of residual N_2O with specific pairwise ratios (Jinuntuya-Nortman et al., 2008; Webster and Hopkins, 1996; Yamagishi et al., 2007).

Nitrogen and oxygen isotope ratios of N_2O are often disregarded, due to lower potential for N_2O source identification as compared to ^{15}N-SP. However, we believe that the use of both isotope approaches should strengthen the conclusions from ^{15}N-SP and reveal additional isotope effects (Fig. 1).

The aim of the current study is to improve our understanding regarding the effects of key environmental variables (oxygenation, temperature, NH_4^+ concentrations) on N_2O production and emission rates. More specifically using nitrogen and oxygen isotope ratios as well as ^{15}N-SP of N_2O should allow deciphering the different producing and consuming pathways under these different conditions. In order to achieve this, the nitrifying biomass of a submerged fixed-bed biofilm reactor was investigated. The research questions addressed are: i) Does the nitrifying biomass emit N_2O and what are the producing pathways at play?; ii) Do oxygenation, temperature, and NH_4^+ concentration alter the N_2O emissions, and what are the involved processes. We hypothesize that the isotope signature of N_2O allows identifying the N_2O origins and the assessment of pathway contribution to N_2O emissions. The results of this study should improve the mechanistic understanding as well as improved prediction of N_2O emissions from WRRFs, currently suffering from high uncertainty.
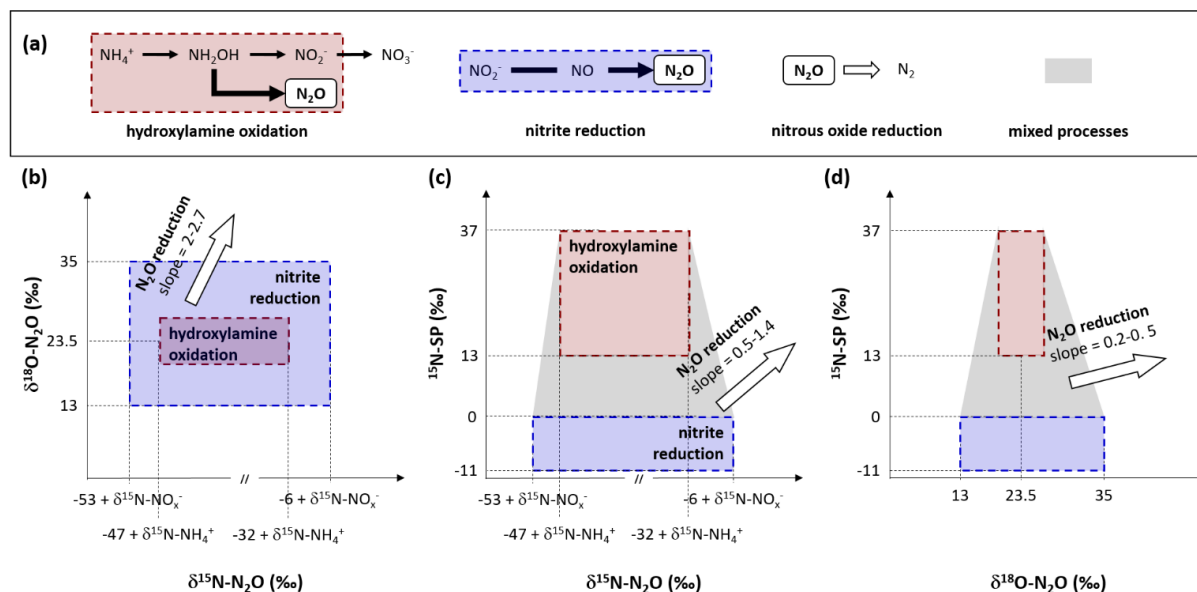
Figure 1: N$_2$O producing and consuming pathways at play during nitrification and denitrification.

2 Material and methods

2.1 Experimental setup for nitrifying experiments

Experiments were carried out with colonized polystyrene beads (diameter 4 mm) sampled from the nitrification biologically active filters (BAF) of a domestic WRRF (Seine Centre, France). In this WRRF, wastewater (240,000 m^3 d^{-1}) passes through a pre-treatment stage, followed by a physicochemical decantation, and tertiary biological treatment. The latter is composed of three biofiltration processes; (i) carbon elimination (24 Biofor®), (ii) nitrification (29 Biostyr®), and (iii) denitrification (12 Biofor®). Nitrifying Biostyrs® are submerged fixed-bed biofilm reactors with a unitary section of 111 m^2 and a filter bed of 3 m high. This unit is operated to receive a nominal load of 0.7 kg NH$_4^+$-N m^{-3} d^{-1}.

A lab-scale reactor with a working volume of 9.9 L (colonized Biostyrene® beads and interstitial volume) and a headspace of 1.4 L was operated in continuous down-flow counter-current mode for seven weeks. Mass flow meters (F-201CV, Bronkhorst, France) sustained the inflow gas rate at 0.5 L min^{-1}. A peristaltic pump (R3425H12B, Sirem, France) pumped feeding solution from a feeding tank into the reactor at 0.2 L min^{-1}, in order to maintain a hydraulic retention time (HRT) of 27.8 ± 0.6 min. A water jacket monitored by a cryogenic regulator (WK 500, Lauda, Germany) controlled the reactor temperature. The feeding solution consisted of ammonium chloride (NH$_4$Cl) as substrate, monobasic potassium phosphate (KH$_2$PO$_4$) as phosphorus source for bacterial growth, and sodium hydrogen carbonate (NaHCO$_3$) as pH buffer and inorganic carbon source in 100 or 150 L of tap water.

The influence of environmental conditions on the ammonium oxidation rates and the N_2O emissions from various combinations of oxygenation levels, temperatures and ammonium concentrations were tested in twenty-four experiments (Tables 1 and S1). The oxygenation tests consisted of mixing compressed air and pure nitrogen gas to reach 0 to 21 % O_2 in the gas mixture (Fig. S1a). They were performed at five substrate concentrations and at a temperature between 19.2 and 20.6 °C. The temperature
105   tests consisted of cooling the feeding solution directly in the feeding tank (22.3 to 13.5 °C), with an inflow ammonium concentration of 19.9-21.1 mg NH_4^+-N L^{-1}. At temperatures ranging from 18.8 to 19.9 °C, the ammonium concentration tests consisted of an increase (6.2, 28.6 and 62.1 mg NH_4^+-N L^1) and a decrease (56.1, 42.9, 42.7 and 20.2 mg NH_4^+-N L^{-1}) in the NH_4^+ concentrations in the feeding solution. An optimal oxygenation level was imposed for both tests (Figs. S1b and c). Sampling started after at least one hydraulic retention time (28 ±1 min).

110   **Table 1. Ranges of environmental conditions tested.**

tests	inflow [NH_4^+]	inflow gas rate	O_2 in gas mixture	temperature
	mg N L^{-1}	*L min^{-1}*	*%*	*°C*
oxygenation	20.2 - 37.3	0.4 - 0.57	0 - 21	19.2 - 20.6
temperature	20.2 - 21.1	0.5	21	13.5 - 22.3
inflow [NH_4^+]	6.2 - 62.1	0.5, 0.57	21	19.0 - 20.3

2.2 Reactor monitoring, sampling and concentrations analysis

Dissolved oxygen, temperature (Visiferm DO Arc 120, Hamilton, Switzerland) and pH (H8481 HD, SI Analytics, France) were continuously measured at the top of the reactor and data were recorded at 10 second intervals. The N_2O concentration was continuously analyzed by an infrared photometer (Rosemount™ X-STREAM X2GP, Emerson, Germany) in outflow
115   reactor gas after drying through a condenser and a hydrophobic gas filter (0.2 µm). Minute averages are used for monitored data hereafter. Gas samples were taken for N_2O isotopic signature determination by outlet gas pipe derivation into a sealed glass vial of 20 ml. The vial was first flushed with the sampling gas for > 45 sec prior to 1-5 min sampling. Gas samples were then stored in the dark at room temperature until analysis.

The feeding solutions were characterized from 1 to 5 samples collected in the feeding tank. For each tested condition, the
120   outflow was characterized within 5 days from 1 to 14 samples immediately filtered through a 0.2 µm syringe filter and stored at 4 °C. Ammonium was analyzed using the Nessler colorimetric method, according to AFNOR NF T90-015 (DR 2800, Hach, Germany). Nitrite and nitrate were measured by ionic chromatography (IC25, Dionex, USA).

2.3 Stable isotope measurements

Atmospheric N_2 and Vienna Standard Mean Ocean Water (VSMOW) are the references used for the nitrogen and oxygen
125   isotopes ratios, respectively, expressed in the conventional δ-notation, in per-mil (‰). Nitrogen and oxygen isotope ratios of

nitrate and nitrite were determined separately following a modified protocol of McIlvin and Altabet (McIlvin and Altabet, 2005; Semaoune et al., 2012). Nitrogen isotope ratios of ammonium were determined following the protocol of Zhang et al. (2007). These methods consist in the conversion of the substrate (ammonium or nitrite or nitrate) into dissolved N_2O. The $\delta^{15}N$ and $\delta^{18}O$ values of N_2O and ^{15}N site preference (^{15}N-SP) values were determined using an isotope ratio mass spectrometer

130　(IRMS, DeltaVplus; Thermo Scientific) in continuous-flow with a purge and trap system coupled with a Finnigan GasBench II system (Thermo Scientific). The method was calibrated with combination of nitrate or ammonium standards (USGS-32, $\delta^{15}N$-NO_3^- = 180 ‰, $\delta^{18}O$-NO_3^- = 25.7 ‰; USGS-34, $\delta^{15}N$-NO_3^- = -1.8 ‰, $\delta^{18}O$-NO_3^- = -27.9 ‰ and USGS-35 $\delta^{15}N$-NO_3^- = 2.7 ‰, $\delta^{18}O$-NO_3^- = 57.5 ‰; or IAEA-N1, $\delta^{15}N$-NH_4^+ = 0.4 ‰, IAEA-305A, $\delta^{15}N$-NH_4^+ = 39.8 ‰, USGS-25, $\delta^{15}N$-NH_4^+ = -30.4 ‰). Linearity of the analysis was checked with international standards (IAEA-NO-3, $\delta^{15}N$-NO_3^- = 4.7 ‰, $\delta^{18}O$-NO_3^- =

135　25.6 ‰; or IAEA-N2, $\delta^{15}N$-NH_4^+ = 20.3 ‰). The precision was 0.8 ‰, 1.5 ‰ and 2.5 ‰ for $\delta^{15}N$, $\delta^{18}O$, and ^{15}N-SP, respectively.

2.4 Data processing and statistics

The effects of environmental conditions on nitrification were assessed from 4 indices. The ammonium oxidation rate (AOR) was estimated in each experiment for time $\geq$ 1 HRT from the difference between influent and effluent NH_4^+ concentrations

140　multiplied by the liquid flow rate (kg NH_4^+-N m^{-3} d^{-1}). The nitrification efficiency was defined as the ratio between AOR and influent ammonium load. The N_2O emission rate (N_2O-ER) was calculated by multiplying the measured N_2O concentration by the gas flow rate (mg N_2O-N min^{-1}). The N_2O emission factor (N_2O-EF) was defined as the ratio between N_2O-ER and AOR (% of oxidized NH_4^+-N).

Statistical analysis were performed using the R software (R Core Team, 2014). The value of 0.05 was used as significance

145　level for spearman correlations (*cor.test* function) and linear regressions (*lm* function). *Adjusted r²* was provided as *r²* for the latter.

2.5 Estimation of nitrogen isotope ratio in N_2O

As shown in Fig. 1, the pairwise relationships between $\delta^{15}N$, $\delta^{18}O$ and ^{15}N-SP assist the determination of the producing and consuming pathways at play. The N atoms that compose the N_2O molecule originate from NH_4^+ molecules when produced by

150　hydroxylamine oxidation, while originating from the N atoms of NO_3^- or NO_2^- molecules when produced by nitrite reduction (NO_x^- molecules). However, the nitrogen isotope ratio of N_2O does not equal those of its substrates as it depends on isotope effects associated to each reaction step of N_2O producing process.

Several equations enable to approximate the isotope effect and its effect on the isotope ratios of substrate and product pools involved in a reaction. These equations vary according to the assumptions made on the system boundaries (Denk et al., 2017).

155　The nitrifying reactor used in this study can be described as an open-system continuously through by an infinite substrate pool with constant isotopic composition. A small amount of the infinite substrate pool is transformed into a product pool or a

residual substrate pool when flowing through the system. Therefore, the N isotope ratios of the residual substrate pool can be approximated from the following Eq. (1) (Denk et al., 2017; Fry, 2006):

$$\delta^{15}N\text{-}NH_4^+{}_{,out} \approx \delta^{15}N\text{-}NH_4^+{}_{,in} - (1-f) \times \varepsilon_{ao} , \tag{1}$$

160 Where f is the remaining substrate fraction leaving the reactor (i.e. remaining fraction of ammonium), ranging from 0 to 1 (0-100 in %), and ε_{ao} the N isotope enrichment factor associated with ammonium oxidation. In their review, Denk et al. (2017) reported a mean value of -29.6 ± 4.9 ‰ for ε_{ao}. Therefore, $\delta^{15}N$ is higher for residual than initial substrate pool ($\delta^{15}N\text{-}NH_4^+{}_{,in}$ < $\delta^{15}N\text{-}NH_4^+{}_{,out}$; where 'in' and 'out' represent inflow and outflow, respectively). Consequently, the pool of product is depleted in heavier isotope (i.e. nitrite and nitrate hereafter defined as NO_x^- pool; $\delta^{15}N\text{-}NO_x^-{}_{,in}$ > $\delta^{15}N\text{-}NO_x^-{}_{,out}$). It can be estimated from

165 Eq. (2):

$$\delta^{15}N\text{-}NO_x^-{}_{,p} \approx \delta^{15}N\text{-}NH_4^+{}_{,in} + f \times \varepsilon_{ao} , \tag{2}$$

Where $\delta^{15}N\text{-}NO_x^-{}_{,p}$ is the nitrogen isotope ratio of the product pool produced by nitrification. The nitrogen isotope ratio of the overall NO_x^- exiting the reactor ($\delta^{15}N\text{-}NO_x^-{}_{,out}$), which results of mixing between initial and produced NO_x^- pools, can be estimated from Eqs. (3) and (4):

$$170 \quad \delta^{15}N\text{-}NO_x^-{}_{,in} = \frac{(\delta^{15}N\text{-}NO_2^-{}_{,in} \times [NO_2^-]_{in} + \delta^{15}N\text{-}NO_3^-{}_{,in} \times [NO_3^-]_{in})}{([NO_3^-]_{in} + [NO_2^-]_{in})} , \tag{3}$$

$$\delta^{15}N\text{-}NO_x^-{}_{,out} \approx \frac{(\delta^{15}N\text{-}NO_x^-{}_{,in} \times ([NO_3^-]_{in} + [NO_2^-]_{in}) + \delta^{15}N\text{-}NO_x^-{}_{,p} \times f \times [NH_4^+]_{in})}{([NO_3^-]_{in} + [NO_2^-]_{in} + f \times [NH_4^+]_{in})} , \tag{4}$$

Whatever the considered system, the net isotope effect of sequential or branched reactions can be approximated from the Δ method that consists in the difference between $\delta^{15}N$ of product and substrate (Denk et al., 2017). Therefore, the nitrogen isotope ratio of N_2O produced by hydroxylamine oxidation or nitrite reduction can be estimated from Eq. (5), with the underlying

175 assumptions that the initial amount of N_2O is negligible as compared to the amount of produced N_2O.

$$\delta^{15}N\text{-}N_2O \approx \delta^{15}N_s + \Delta , \tag{5}$$

Where $\delta^{15}N_s$ is the nitrogen isotope ratio of N_2O substrate, which can range between the nitrogen isotope ratios measured or estimated for inflow and outflow NH_4^+ and NO_x^- (Eqs. (1-4)). Net isotope effects (Δ) from literature were used for each N_2O producing pathway (Denk et al., 2017; Toyoda et al., 2017).

180 3 Results and Discussion

Changes in pH, ammonium, nitrite and nitrate concentrations confirmed nitrifying activity in the reactor system (Text S1, Table S2, Fig. S2). Over the range of tested conditions, the ratio between ammonium oxidation rate and influent ammonium concentrations ranged from 10 to 82 %, never exceeding 40 % for suboptimal nitrifying conditions imposed during oxygenation

and temperature tests. Within the tested oxygen, temperature and ammonia conditions, the resulting range of ammonium
185   oxidation rates, N_2O emission rates and factors decreased in the order ammonium concentration, oxygenation level and
temperature.

3.1 Isotope composition ranges of N_2O produced by hydroxylamine oxidation and nitrite reduction

Ranges of $\delta^{15}N$ for N_2O produced by different processes were hypothesized from Eqs. (1-5) for pairwise relationships with
reviewed data of $\delta^{18}O$ and ^{15}N-SP. To this aim, measurements of isotope ratios of the different nitrogen species were required.
190   The $\delta^{15}N$ of inflow ammonium, nitrite and nitrate were -3 ± 0.1 ‰ (n = 3), -15 ± 0.1 ‰ (n = 2), 6.9 ± 0.3 ‰ (n = 3), respectively
during ammonium concentration experiments (Fig. S2). The $\delta^{15}N$ of outflowing NH_4^+ and NO_x^- were estimated from Eqs. (1-4)
with f = 0 or 1, ε_{ao} = -30 ‰, the highest $[NH_4^+]_{in}$ (62.1 mg N L^{-1}) and the lowest $[NO_x^-]_{in}$ (1.4 mg N L^{-1}). They ranged from -3
to 27 ‰ and from -32 to 7 ‰, respectively.

Prior to pairwise comparisons with $\delta^{18}O$ and ^{15}N-SP, ranges of $\delta^{15}N$ values for N_2O produced by the hydroxylamine oxidation
195   and nitrite reduction pathways were estimated from Eq. (5). The net isotope effect of N_2O production by ammonium oxidation
via hydroxylamine can be estimated by combining the isotope effects of ammonium oxidation and hydroxylamine oxidation
to N_2O. The net isotope effect associated to the ammonium oxidation to nitrite ranges from -38.2 to -14.2 ‰ (Casciotti et al.,
2003) and can approximate the nitrogen isotope ratio of hydroxylamine transitory produced. The isotope effect related to
hydroxylamine oxidation to N_2O ranging from -26.3 to 5.7 ‰ (Sutka et al., 2003, 2006), the net isotope effect of N_2O
200   production by ammonium oxidation via hydroxylamine can range from -64.5 ‰ (-26.3 + (-38.2)) to -8.5 ‰ (5.7 + (-14.2)).
This method provided a broad range of $\delta^{15}N$ values, from -68 to 19 ‰, for N_2O produced by hydroxylamine oxidation that
encompassed the values proposed by others (-46.9 and -32.6 ‰; Sutka et al., 2006; Yamazaki et al., 2014).

A higher net nitrogen isotope effect for nitrite reduction than hydroxylamine oxidation pathway was observed for N_2O
production (Figs. 2a and b). Prior being reduced to N_2O through the nitrite reduction pathway, NO_x^- was mainly derived from
205   ammonium oxidation in the nitrifying system (Eqs. (1-4)). Consequently, the $\delta^{15}N$ of N_2O produced by nitrite reduction ranged
from -85 ‰ (-53 + (-32)) to 1 ‰ (-6 + 7). This is consistent with previous findings reporting $\delta^{15}N$-N_2O between -112 and -48 ‰
for nitrifier-denitrifying systems (Mandernack et al., 2009; Pérez et al., 2006; Yamazaki et al., 2014; Yoshida, 1988). However,
a similar range of nitrite-derived $\delta^{15}N$-N_2O is suggested for nitrifiers and denitrifiers, because ammonium oxidation influences
both processes in the system used in this study.

210   Pairwise comparisons of $\delta^{15}N$, $\delta^{18}O$ and ^{15}N-SP estimates of the different experiments are presented in Fig. 2. These
comparisons provided ranges of plausible isotope compositions for N_2O produced by nitrifying or denitrifying bacteria through
the hydroxylamine oxidation and nitrite reduction pathways (red and blue boxes, respectively). The measured N_2O isotope
compositions were compared to these estimates to identify the N_2O producing and consuming pathways likely at play in
oxygenation, temperature, and ammonium concentration tests.

215   This approach suggests that the nitrite reduction pathway was the main contributor to the N_2O emissions. Heterotrophic denitrification likely influenced the N_2O emissions, as shown by oxygen isotope ratios higher than 35 ‰ (Snider et al., 2013) (Figs. 2a and c). However, this conclusion depends highly on $\delta^{18}O$-N_2O ranges. Furthermore, the application of atmospheric oxygen $\delta^{18}O$ (23.5 ‰; Kroopnick and Craig, 1972) to estimate the oxygen isotope ratio of N_2O produced by hydroxylamine oxidation remains uncertain since respiratory activity and air stripping might drive isotopic fractionations and increase the

220    $\delta^{18}O$ of residual dissolved oxygen (Nakayama et al., 2007). To date, the oxygen isotope fractionation related to air stripping is lacking. Note that this estimate relies on the assumption that there is no accumulation of NH_2OH and that its oxidation to N_2O occurs before or independently of its oxidation to NO_2^-.
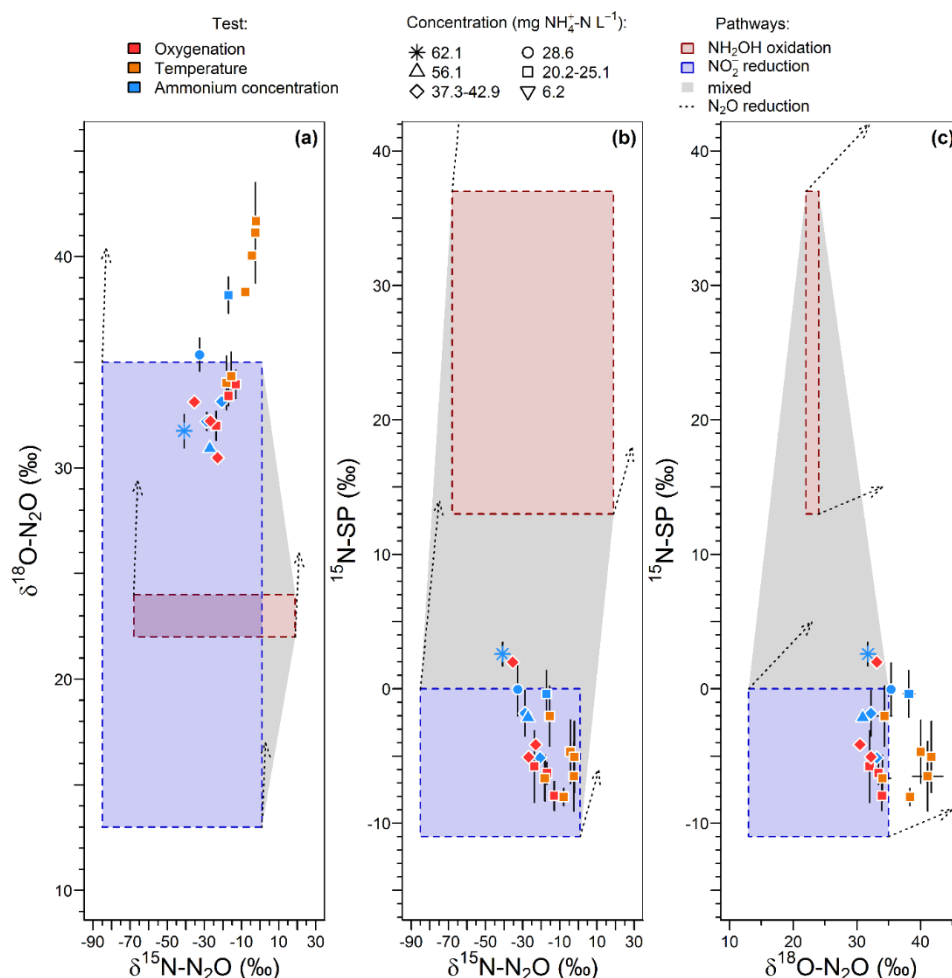

Figure 2: Interpretation maps of the isotope signature of N_2O. Schematic maps of (a) $\delta^{15}N$-$\delta^{18}O$, (b) $\delta^{15}N$-^{15}N-SP, and (c) $\delta^{18}O$-^{15}N-SP. The red and blue squares show the range of the data for N_2O produced by 'hydroxylamine oxidation' and 'nitrite reduction', respectively. The shaded area represents mixing of N_2O produced by these pathways. The N_2O reduction increases $\delta^{15}N$, $\delta^{18}O$, and ^{15}N-SP with slopes characterizing the pairwise relationships.

3.2 The effect of oxygen limitation on the N$_2$O producing pathways

Ammonium concentrations decreased from 20.2-37.3 to 11.4-31.1 mg N L^{-1}; with 45 to 89 % of the inflow ammonium
225   remaining in the outflow during the oxygenation tests (Fig. S1d). The cumulated concentrations of NO$_2^-$ and NO$_3^-$ ([NO$_x^-$])
increased from 2.4-4.1 to 4.7-11 mg N L^{-1} between inflow and outflow and were composed by at least 74 and 82 % of NO$_3^-$,
respectively.

The oxygenation level had contrasting effects on ammonium oxidation rates, and N$_2$O emission rates and factors (Figs. 3a-c).
Between an oxygenation of 0 to 10.5 % O$_2$ in the gas mixture, ammonium oxidation rates were low and stable (1.1 ± 0.5 mg
230   NH$_4^+$-N min^{-1}), with N$_2$O emission rates and factors increasing from 0.35 10^{-3} to 1.6 10^{-3} mg N min^{-1} and from 0.05 to 0.16 %,
respectively. At oxygenation levels from 10.5 to 21 % O$_2$, the ammonium oxidation rates increased from 0.9 ± 0.2 to 2.1 ± 0.4
mg N min^{-1}, with N$_2$O emission rates remaining stable at 1.2 10^{-3} ± 0.6 10^{-3} mg N min^{-1} and the emission factors decreasing
from 0.15 ± 0.03 to 0.06 ± 0.03 %.

The ^{15}N-SP varied between -9 to 2 ‰ over the range of imposed oxygenation levels, with a marked increase when oxygenation
235   increased from 16.8 to 21 % O$_2$ (Fig. 3d). A similar marked change in nitrogen and oxygen isotope ratios of N$_2$O (decrease
and increase, respectively) was observed when oxygenation increased from 16.8 to 21 % O$_2$ (Figs. 3e and f). The ^{15}N-SP values
were close to the range of -11 to 0 ‰ reported for N$_2$O produced by nitrifying or denitrifying bacteria (Toyoda et al., 2017;
Yamazaki et al., 2014). This suggests an important contribution of the NO$_2^-$ reduction pathway to N$_2$O emissions. The ^{15}N-SP
dynamics between and variations within the oxygenation levels suggest a higher amount of N$_2$O reduced to N$_2$ at 4.2 than 16.8
240   % O$_2$. The reduction of N$_2$O to N$_2$ can increase the ^{15}N-SP of residual N$_2$O (Mothet et al., 2013). In heterotrophic denitrifying
bacteria however, the nitrous oxide reductase involved in this reaction is highly sensitive to inhibition by oxygen (Betlach and
Tiedje, 1981; Otte et al., 1996). This might explain the decrease in ^{15}N-SP from -3.8 ± 4.4 ‰ to -7.2 ± 1.7 ‰ when O$_2$ increased
from 4.2 to 16.8 %. This is also consistent with a possible onset of anoxic microsites within the reactor biomass more likely at
4.2 than 16.8 % O$_2$. Finally, the N$_2$O reduction to N$_2$ likely explains the overall decrease in N$_2$O emission between 16.8 and 0
245   % O$_2$ (Fig. 3b).

In general the N$_2$O reduction to N$_2$ is accompanied by an increase in nitrogen and oxygen isotope ratios of N$_2$O (Ostrom et al.,
2007; Vieten et al., 2007). However, our results show a decrease in δ^{15}N-N$_2$O and the δ^{18}O-N$_2$O remained stable between 30.5
and 34.7 ‰ when the N$_2$O reduction is thought to increasingly constraint the N$_2$O isotopocules with decreasing O$_2$ from 16.8
to 4.2 % (Figs. 3e and f). The independence of samples taken during the oxygenation test can explain this. The N$_2$O sampled
250   at 4.2 % O$_2$ is not the N$_2$O produced at 16.8 % O$_2$ then partially reduced. Before being reduced, the N$_2$O produced at different
oxygen levels has an isotope composition likely controlled by the reaction rates and the resulting net isotope effect. For
example, Vieten et al. (2007) reported such control of isotope fractionation factors by the oxygenation levels through the
control of N$_2$O reduction rate. Additionally, with δ^{18}O below 35 ‰ for all but one experiment the oxygenation tests did not
provide evidence for denitrifier contribution to N$_2$O emissions, likely due to oxygen-exchange with water (Snider et al., 2015,
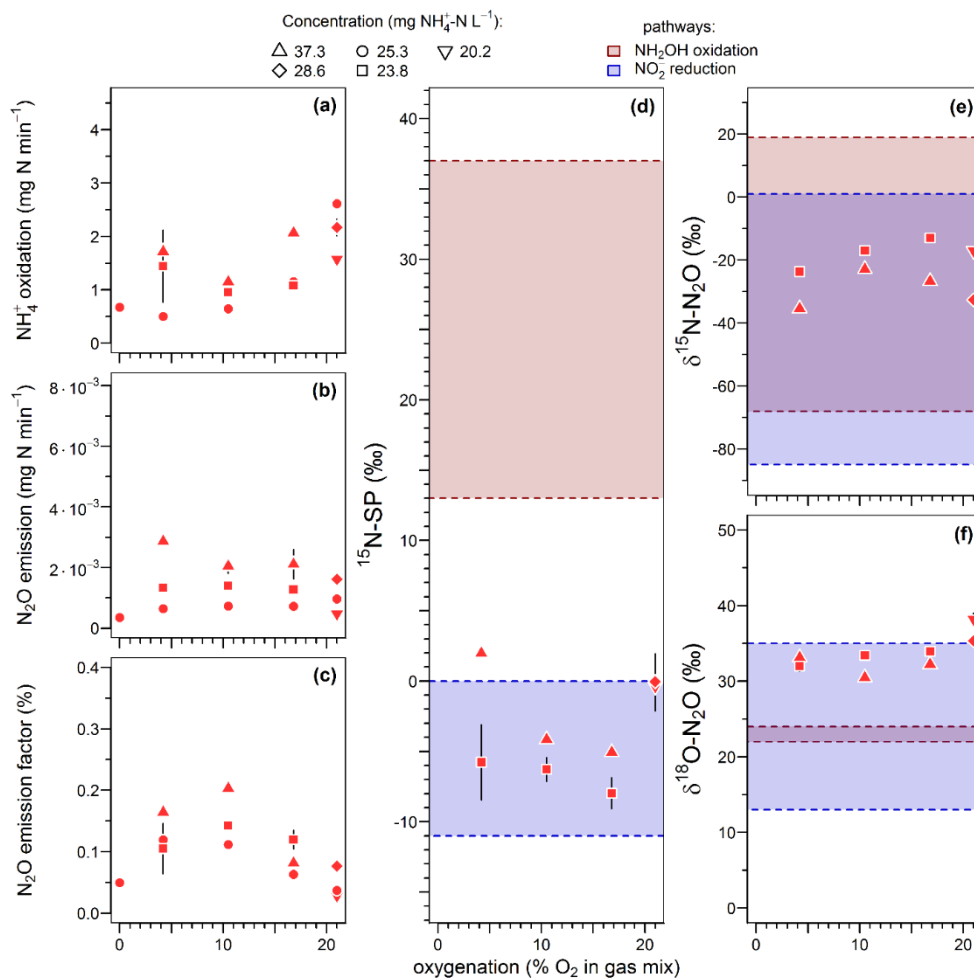255   2012, 2013).

Figure 3: Effect of oxygenation level on (a) the ammonium oxidation rate, (b) the nitrous oxide emission rate, (c) the N₂O emission factor, and (d) the nitrogen isotopomer site preference, (e) the nitrogen isotope ratio, and (f) the oxygen isotope ratio of N₂O. Average and standard deviation (error bars) are calculated for the steady-state conditions.

3.3 Difference in temperature dependency of hydroxylamine and ammonium oxidizers as driver of hydroxylamine oxidation contribution to N₂O emissions

Ammonium concentrations decreased from 6.2-62.1 to 0.9-54.1 mg N L⁻¹; from 18 to 79 % of the inflow ammonium remaining in the outflow during the temperature and ammonium concentration tests (Figs. S1e and f). This remaining fraction was

260 positively correlated to ammonium concentrations ($r = 0.96$), and negatively correlated to temperature within the lower range of values (61-67 %; $r = -0.94$). The cumulated concentrations of NO_2^- and NO_3^- ([NO_x^-]) increased from 1.4-6.1 to 5.1-19.6 mg N L⁻¹ between inflow and outflow and were composed by at least 74 and 91 % of NO_3^-, respectively. Noticeably, the nitrite concentrations in the outflow linearly increased with temperature ($r^2 = 0.95$; Fig. S1h).

An increase in temperature and inflow ammonium concentrations both positively influenced the rates of NH_4^+ oxidation and

265   N_2O emissions and the emission factor (Fig. 4). The NH_4^+ oxidation rate linearly increased from 1.3 to 1.5 mg NH_4^+-N min^{-1} with temperature ($r = 0.89$; Fig. 4a) and increased from 0.97 to 3.49 mg NH_4^+-N min^{-1} with a tenfold increase in the inflow ammonium concentration ($r = 0.82$; Fig. 4b). These positive correlations are well known in the temperature range investigated here and are likely due to enhanced enzymatic activity (Groeneweg et al., 1994; Kim et al., 2008; Raimonet et al., 2017). Similarly, the N_2O emission rates increased from 80.4 10^{-6} to 2.5 10^{-3} mg N_2O-N min^{-1}, and from 83.6 10^{-6} to 6.2 10^{-3} mg

270   N_2O-N min^{-1} upon changes in temperature and ammonium concentrations, respectively. These results are in agreement with positive correlations between N_2O emissions with temperature and ammonium concentration observed from modelling and experimental studies on partial nitrification and activated sludge systems (Guo and Vanrolleghem, 2014; Law et al., 2012a; Reino et al., 2017). Altogether this confirms a correlation between the N_2O emission rates and to the ammonium oxidation rates. Interestingly, the increase in N_2O emission factor indicates a stronger effect of temperature and ammonium concentration

275   on the N_2O emission rate than on NH_4^+ oxidation. The N_2O emission factors increased from 0.07 to 0.16 %, and from 0.01 to 0.29 % with temperature and inflow ammonium concentration, respectively ($r > 0.94$; Figs. 4e and f). Both experiments suggest that the increase in N_2O emissions result from the increasing production of N_2O by hydroxylamine oxidation or nitrite reduction in combination with a slow rate of or absence of N_2O reduction to N_2. Furthermore, no nitrite accumulation was observed with increasing ammonium oxidation rate (Fig. S1i). Therefore, in the case where N_2O emission results mainly from the nitrite

280   reduction pathway, this suggests that the nitrite reduction pathway is more responsive to the increasing ammonium oxidation rate than the nitrite oxidation pathway.
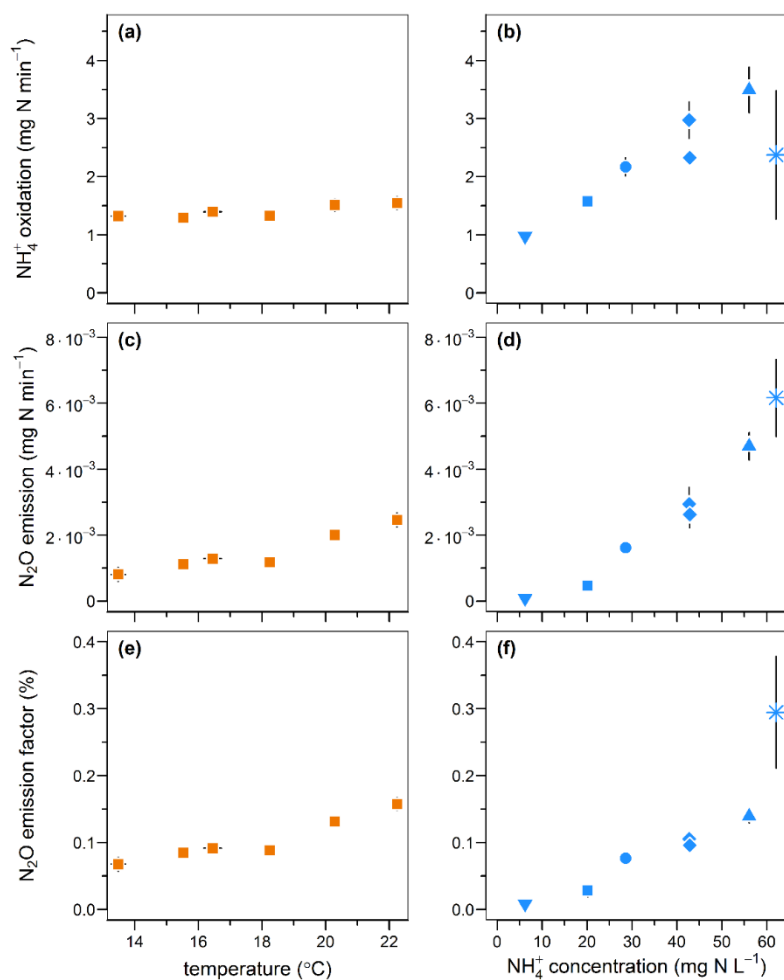
Figure 4: Effect of temperature and inflow ammonium concentration on (a, b) the ammonium oxidation rate, (c, d) the nitrous oxide emission rate, and (e, f) the N₂O emission factor.

The range of nitrogen isotopomer site preference observed during the temperature and concentration tests (from -8 to 2.6 ‰) was similar to those measured during the oxygenation tests; confirming the high contribution of the nitrite reduction pathway to N₂O emissions (Fig. 5a). This is consistent with previous findings based on the ^{15}N-SP of N₂O emitted from aerobic activated sludge (Toyoda et al., 2011; Wunderlin et al., 2013). Furthermore, the ^{15}N-SP increased with temperature and ammonium concentration for temperatures between 13.5 and 19.8 °C. Similarly, Wunderlin et al. (2012, 2013) observed an increase in ^{15}N-SP from -1.2 to 1.1 ‰ when inflow [NH_4^+] increased from 9 to 15 mg N L^{-1}. They also observed 3-6 ‰ decreases in ^{15}N-SP over the course of ammonium oxidation experiments and suggested that NH_2OH oxidation contribution to N₂O production increased when conditions of NH_4^+ in excess, low NO_2^- concentrations and high nitrogen oxidation rate occur simultaneously. Our data suggest that temperature mainly controlled the change in N₂O producing pathways (Fig. 5a). This is consistent with the observation of Groeneweg et al. (1994) showing that temperature rather than ammonium concentration influenced the

13

ammonium oxidation rate. The ^{15}N-SP increased from -6.5 to 2.6 ‰ with increasing temperature from 13.5 to 19.8 °C (Fig. 5a). This ^{15}N-SP increase may either result from an increase in the N_2O production by the hydroxylamine oxidation pathway or the N_2O reduction to N_2. Since an optimal oxygenation level was imposed and increased emissions were observed, the

295 increasing ^{15}N-SP is more likely due to N_2O production by the hydroxylamine oxidation pathway. Reino et al. (2017) also observed an increase of N_2O emissions for temperature above 15 °C in a granular sludge airlift reactor performing partial nitritation. The authors suggested two hypothesis to explain their results: (i) the difference in the kinetic dependency with temperature of enzymes involved in ammonium and hydroxylamine oxidation; (ii) the temperature dependency of the acid-base equilibrium ammonium-ammonia. The changes in ^{15}N-SP observed here are consistent with the former hypotheses.

300 Hydroxylamine oxidation likely becomes the limiting step at a temperature above 15 °C, while being faster than ammonium oxidation at lower temperature (Fig. 6). At temperature above 15 °C, hydroxylamine therefore accumulates and leads to a higher contribution of the hydroxylamine oxidation pathway to N_2O emissions. It would thus be interesting to determine the temperature dependency of the hydroxylamine oxidase.

The change in nitrous oxide producing and consuming pathways had contrasted effects on the nitrogen and oxygen isotope

305 ratios of nitrous oxide (Figs. 5b and c). The δ^{15}N-N_2O decreased from -2.5 to -40.9 ‰ with an increasing contribution of hydroxylamine oxidation to the N_2O emissions; i.e. when temperature increased from 13.5 to 19.8 °C. This is in contrast with the expected net lower isotope effect for N_2O produced by hydroxylamine oxidation than nitrite reduction and points out that further investigations are needed (Snider et al., 2015; Yamazaki et al., 2014). The changes in δ^{18}O-N_2O were less straightforward; likely influenced by changes in the reaction rates in addition to changes in the contribution of N_2O producing

310 pathways. The values decreased from 41.1 to 34.3 ‰ with an increasing contribution of hydroxylamine oxidation to the N_2O emissions; when temperature increased from 13.5 to 18.2 °C. It decreased linearly from 38.2 to 31.8 ‰ with increasing reaction rate, when inflow ammonium concentration increased from 20.2 to 62.1 mg NH_4^+-N L^{-1} ($r^2 = 0.83$).
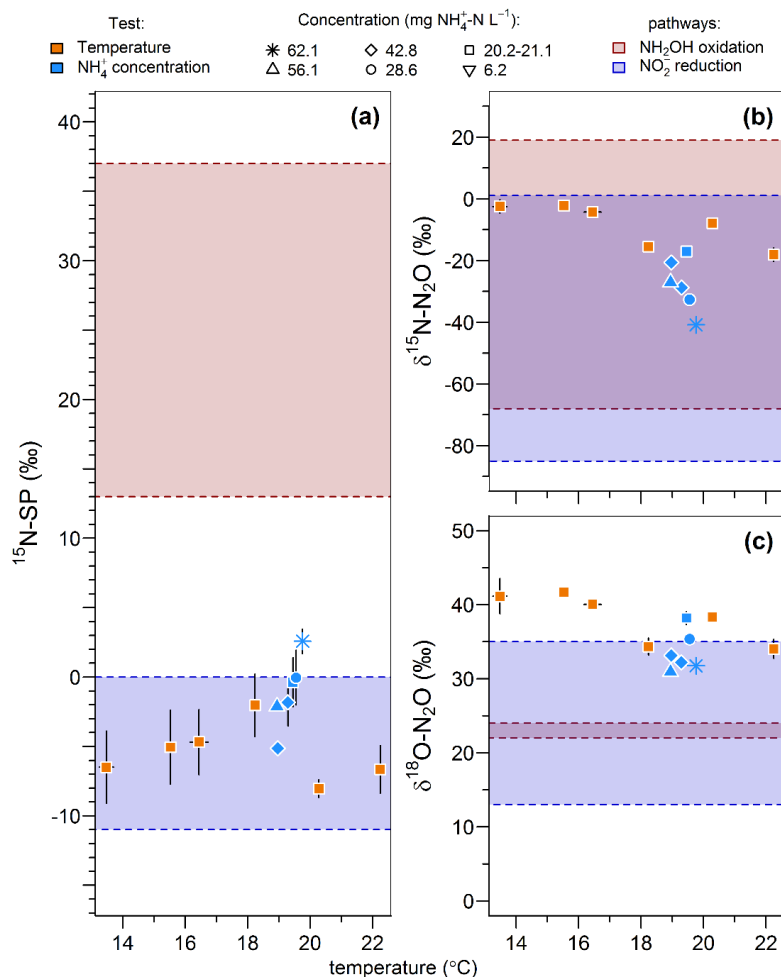
Figure 5: Effect of temperature (orange symbols) and inflow ammonium concentration (blue symbols) on (a) the nitrogen isotopomer site preference, (b) the nitrogen isotope ratio, and (c) the oxygen isotope ratio of N₂O. Average and standard deviation (error bars) are calculated for the steady-state conditions.

3.4 Difference in oxidation and reduction rates of nitrite as driver of nitrite reduction contribution to N₂O emissions

The oxygenation, temperature and ammonium concentration tests revealed a strong control of nitrite oxidizing activity and the

315   contribution of the nitrite reduction pathway to N₂O production. During the oxygenation test, the combination of stable NO_2^- concentrations and higher ^{15}N-SP at 21 % compared to the 10.5-16.8 % O_2 was observed while temperature remained below 20 °C (Figs. S1g and 3d). This is most likely due to higher nitrite oxidation than nitrite reduction rates in response to increasing oxygenation levels to 21 % O_2, which is consistent with the nitrite oxidation step sensitivity to oxygen limitation (Pollice et al., 2002; Tanaka and Dunn, 1982). Additionally, the ^{15}N-SP close to 0 ‰ observed at the highest oxygenation level indicates

320   a decreasing contribution to N₂O production of nitrite reduction over hydroxylamine oxidation pathway. The highest

oxygenation level thus limits the reduction pathways (i.e. NO_2^- reduction to N_2O and N_2O reduction to N_2) while favoring the ammonium and nitrite oxidation pathways.
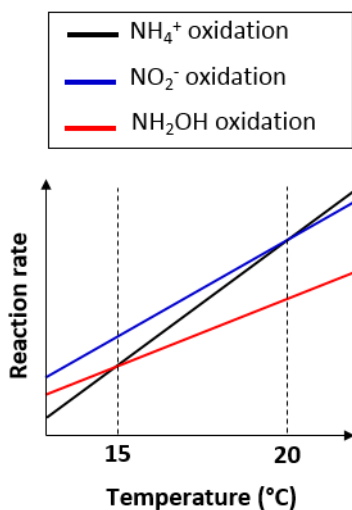

Figure 6: Scheme of the difference in temperature dependency of the reactions involved in nitrification.

During the temperature and ammonium concentration tests, the contribution of the hydroxylamine oxidation pathway to N_2O emissions exponentially increased with temperature between 15 and 20 °C (Sect. 3.2) and decreased in favor of the nitrite

325 reduction pathway when temperature exceeded 20 °C (Fig. 5a). The ^{15}N-SP was low when temperature exceeded 20 °C (-7.3 ± 1 ‰), while being higher than -5 ‰ (-1.3 ± 2.4 ‰) when temperature ranged from 18.2 to 19.8 °C. At temperatures above 20 °C, ammonium oxidation rates exceed nitrite oxidation rates (Fig. 6; Kim et al., 2008; Raimonet et al., 2017). This explains most likely the increased contribution of the nitrite reduction pathway to N_2O emission, as more nitrite becomes available for nitrifier-denitrification and/or denitrification. As little nitrite accumulated (Fig. S1h), lower rates of nitrite

330 consuming than producing processes can be inferred (nitrite reduction and oxidation vs. ammonium oxidation). Additionally, values of $\delta^{18}O > 35$ ‰ measured during these tests suggest a significant contribution of denitrifiers to N_2O emissions (Snider et al., 2013). This seems to occur at the lowest hydroxylamine oxidation contribution to N_2O production; below 18°C and at 20.3 °C. Furthermore, the denitrifiers were impacted to a larger extend by temperature than ammonium concentration.

4 Conclusion

335 Our results demonstrated that whatever the imposed conditions, the nitrifying biomass produced N_2O and nitrite reduction remained the main N_2O producing pathway. The N_2O emissions were sensitive to oxygenation, temperature, and NH_4^+ concentration likely due to control of enzymatic activities. The use of N_2O isotopocules confirmed the processes that control N_2O emissions under oxygenation constrain and improved the knowledge of processes that control N_2O under temperature constrain. Among the environmental variables tested, temperature appears to be the main control on N_2O producing pathways

Biogeosciences Open Access

Discussions

EGU

340   under nitrifying conditions, due to its dissimilar effects on ammonium and nitrite oxidizing activities. Ranges of optimal temperature for nitrification and limited N_2O emissions can be recommended. The combination of low N_2O emissions and high nitrification rates would occur close to 15 °C. From 15 to 20 °C, increasing nitrification rate increase the N_2O emissions by the hydroxylamine oxidation pathway. Above 20 °C, an increasing nitrification rate increases the N_2O emissions via the nitrite reduction pathway.

345 **Supplementary material**

Additional information about the nitrifying activity of the biomass, the experimental conditions, and the time series of ammonium oxidation experiments.

Author contribution

JF, AF and MSp designed the experiments with contributions from GH, MSe and AML. GH, JF and LL carried the experiments
350   out. GH performed the stable isotope measurements with contribution from VV and interpreted them with contribution from MSe. GH and JF processed the data. GH, JF and AML prepared the manuscript with contributions from all co-authors.

Competing interests

The authors declare that they have no conflict of interest.

Acknowledgements

References

360   Andersson, K. K. and Hooper, A. B.: O_2 and H_2O are each the source of one O in NO_2^- produced from NH_3 by Nitrosomonas: ^{15}N-NMR evidence, FEBS Lett., 164(2), 236–240, doi:10.1016/0014-5793(83)80292-0, 1983.

Betlach, M. R. and Tiedje, J. M.: Kinetic explanation for accumulation of nitrite, nitric oxide, and nitrous oxide during bacterial denitrification., Appl. Environ. Microbiol., 42(6), 1074–84, 1981.

Bollon, J., Filali, A., Fayolle, Y., Guerin, S., Rocher, V. and Gillot, S.: N_2O emissions from full-scale nitrifying biofilters,
365   Water Res., 102, 41–51, doi:10.1016/j.watres.2016.05.091, 2016.

Bothe, H., Ferguson, S. J. and Newton, W. E.: Biology of the nitrogen cycle., 2007.

Caranto, J. D., Vilbert, A. C. and Lancaster, K. M.: Nitrosomonas europaea cytochrome P460 is a direct link between nitrification and nitrous oxide emission., Proc. Natl. Acad. Sci. U. S. A., 113(51), 14704–14709, doi:10.1073/pnas.1611051113, 2016.

370 Casciotti, K. L., Sigman, D. M. and Ward, B. B.: Linking diversity and stable isotope fractionation in ammonia-oxidizing bacteria, Geomicrobiol. J., 20(4), 335–353, doi:10.1080/01490450303895, 2003.

Crutzen, P. J., Heidt, L. E., Krasnec, J. P., Pollock, W. H. and Seiler, W.: Biomass burning as a source of atmospheric gases CO, H_2, N_2O, NO, CH_3Cl and COS, Nature, 282(5736), 253–256, doi:10.1038/282253a0, 1979.

Denk, T. R. A., Mohn, J., Decock, C., Lewicka-Szczebak, D., Harris, E., Butterbach-Bahl, K., Kiese, R. and Wolf, B.: The
375 nitrogen cycle: A review of isotope effects and isotope modeling approaches, Soil Biol. Biochem., 105, 121–137, doi:10.1016/j.soilbio.2016.11.015, 2017.

Frame, C. H. and Casciotti, K. L.: Biogeochemical controls and isotopic signatures of nitrous oxide production by a marine ammonia-oxidizing bacterium, Biogeosciences, 7(9), 2695–2709, doi:10.5194/bg-7-2695-2010, 2010.

Fry, B.: Stable Isotope Ecology, Springer-Verlag New York., 2006.

380 Groeneweg, J., Sellner, B. and Tappe, W.: Ammonia oxidation in nitrosomonas at NH_3 concentrations near km: Effects of pH and temperature, Water Res., 28(12), 2561–2566, doi:10.1016/0043-1354(94)90074-4, 1994.

Guo, L. and Vanrolleghem, P. A.: Calibration and validation of an activated sludge model for greenhouse gases no. 1 (ASMG1): prediction of temperature-dependent N_2O emission dynamics, Bioprocess Biosyst. Eng., 37(2), 151–163, doi:10.1007/s00449-013-0978-3, 2014.

385 Heil, J., Liu, S., Vereecken, H. and Brüggemann, N.: Abiotic nitrous oxide production from hydroxylamine in soils and their dependence on soil properties, Soil Biol. Biochem., 84, 107–115, doi:10.1016/J.SOILBIO.2015.02.022, 2015.

Hollocher, T. C., Tate, M. E. and Nicholas, D. J.: Oxidation of ammonia by Nitrosomonas europaea. Definite ^{18}O-tracer evidence that hydroxylamine formation involves a monooxygenase., J. Biol. Chem., 256(21), 10834–10836, 1981.

IPCC: Climate Change 2014: Impacts, Adaptation, and Vulnerability, Organ. Environ., 24(March), 1–44, 2014.

390 Jinuntuya-Nortman, M., Sutka, R. L., Ostrom, P. H., Gandhi, H. and Ostrom, N. E.: Isotopologue fractionation during microbial reduction of N_2O within soil mesocosms as a function of water-filled pore space, Soil Biol. Biochem., 40(9), 2273–2280, doi:10.1016/j.soilbio.2008.05.016, 2008.

Jung, M.-Y., Well, R., Min, D., Giesemann, A., Park, S.-J., Kim, J.-G., Kim, S.-J. and Rhee, S.-K.: Isotopic signatures of N_2O produced by ammonia-oxidizing archaea from soils, ISME J., 8(5), 1115–25, doi:10.1038/ismej.2013.205, 2014.

395 Kampschreur, M. J., Temmink, H., Kleerebezem, R., Jetten, M. S. M. and van Loosdrecht, M. C. M.: Nitrous oxide emission during wastewater treatment, Water Res., 43(17), 4093–4103, doi:10.1016/j.watres.2009.03.001, 2009.

Kim, J.-H., Guo, X. and Park, H.-S.: Comparison study of the effects of temperature and free ammonia concentration on nitrification and nitrite accumulation, Process Biochem., 43(2), 154–160, doi:10.1016/J.PROCBIO.2007.11.005, 2008.

Koba, K., Osaka, K., Tobari, Y., Toyoda, S., Ohte, N., Katsuyama, M., Suzuki, N., Itoh, M., Yamagishi, H., Kawasaki, M.,
400 Kim, S. J., Yoshida, N. and Nakajima, T.: Biogeochemistry of nitrous oxide in groundwater in a forested ecosystem elucidated by nitrous oxide isotopomer measurements, Geochim. Cosmochim. Acta, 73(11), 3115–3133, doi:10.1016/j.gca.2009.03.022, 2009.

Kool, D. M., Wrage, N., Oenema, O., Dolfing, J. and Van Groenigen, J. W.: Oxygen exchange between (de)nitrification intermediates and H_2O and its implications for source determination of NO_3^- and N_2O: a review, Rapid Commun. Mass
405 Spectrom., 21(22), 3569–3578, doi:10.1002/rcm.3249, 2007.

Kroopnick, P. and Craig, H.: Atmospheric oxygen: isotopic composition and solubility fractionation., Science, 175(4017), 54–5, doi:10.1126/science.175.4017.54, 1972.

Law, Y., Ni, B.-J., Lant, P. and Yuan, Z.: N_2O production rate of an enriched ammonia-oxidising bacteria culture exponentially correlates to its ammonia oxidation rate, Water Res., 46(10), 3409–3419, doi:10.1016/j.watres.2012.03.043, 2012a.

410 Law, Y., Ye, L., Pan, Y. and Yuan, Z.: Nitrous oxide emissions from wastewater treatment processes., Philos. Trans. R. Soc. Lond. B. Biol. Sci., 367(1593), 1265–1277, doi:10.1098/rstb.2011.0317, 2012b.

Lewicka-Szczebak, D., Well, R., Köster, J. R., Fuß, R., Senbayram, M., Dittert, K. and Flessa, H.: Experimental determinations of isotopic fractionation factors associated with N_2O production and reduction during denitrification in soils, Geochim. Cosmochim. Acta, 134, 55–73, doi:10.1016/j.gca.2014.03.010, 2014.

415 Mandernack, K. W., Mills, C. T., Johnson, C. A., Rahn, T. and Kinney, C.: The $\delta^{15}N$ and $\delta^{18}O$ values of N_2O produced during the co-oxidation of ammonia by methanotrophic bacteria, Chem. Geol., 267(1–2), 96–107,

Biogeosciences
Discussions

Open Access

EGU

doi:10.1016/J.CHEMGEO.2009.06.008, 2009.

McIlvin, M. R. and Altabet, M. A.: Chemical conversion of nitrate and nitrite to nitrous oxide for nitrogen and oxygen isotopic analysis in freshwater and seawater, Anal. Chem., 77(17), 5589–5595, doi:10.1021/ac050528s, 2005.

420 Mothet, A., Sebilo, M., Laverman, A. M., Vaury, V. and Mariotti, A.: Is site preference of N$_2$O a tool to identify benthic denitrifier N$_2$O?, Environ. Chem., 10(4), 281–284, doi:10.1071/EN13021, 2013.

Nakayama, N., Obata, H. and Gamo, T.: Consumption of dissolved oxygen in the deep Japan Sea, giving a precise isotopic fractionation factor, Geophys. Res. Lett., 34(20), doi:10.1029/2007GL029917, 2007.

Ostrom, N. E., Pitt, A., Sutka, R., Ostrom, P. H., Grandy, A. S., Huizinga, K. M. and Robertson, G. P.: Isotopologue effects

425 during N$_2$O reduction in soils and in pure cultures of denitrifiers, J. Geophys. Res., 112(G2), doi:10.1029/2006JG000287, 2007.

Otte, S., Grobben, N. G., Robertson, L. A., Jetten, M. S. and Kuenen, J. G.: Nitrous oxide production by Alcaligenes faecalis under transient and dynamic aerobic and anaerobic conditions., Appl. Environ. Microbiol., 62(7), 2421–6, 1996.

Pérez, T., Garcia-Montiel, D., Trumbore, S., Tyler, S., Camargo, P. de, Moreira, M., Piccolo, M. and Cerri, C.: Nitrous oxide

430 nitrification and denitrification ^{15}N enrichment factors from Amazon forest soils, Ecol. Appl., 16(6), 2153–2167, doi:10.1890/1051-0761(2006)016[2153:nonadn]2.0.co;2, 2006.

Pollice, A., Tandoi, V. and Lestingi, C.: Influence of aeration and sludge retention time on ammonium oxidation to nitrite and nitrate, Water Res., 36(10), 2541–2546, doi:10.1016/S0043-1354(01)00468-7, 2002.

R Core Team: R: A language and environment for statistical computing, 2014.

435 Raimonet, M., Cazier, T., Rocher, V. and Laverman, A. M.: Nitrifying kinetics and the persistence of nitrite in the Seine river, France, J. Environ. Qual., 46(3), 585–595, doi:10.2134/jeq2016.06.0242, 2017.

Ravishankara, A. R., Daniel, J. S. and Portmann, R. W.: Nitrous oxide (N$_2$O): the dominant ozone-depleting substance emitted in the 21st century., Science, 326(5949), 123–125, doi:10.1126/science.1176985, 2009.

Reino, C., van Loosdrecht, M. C. M., Carrera, J. and Pérez, J.: Effect of temperature on N$_2$O emissions from a highly enriched

440 nitrifying granular sludge performing partial nitrition of a low-strength wastewater, Chemosphere, 185, 336–343, doi:10.1016/j.chemosphere.2017.07.017, 2017.

Semaoune, P., Sebilo, M., Templier, J. and Derenne, S.: Is there any isotopic fractionation of nitrate associated with diffusion and advection?, Environ. Chem., 9(2), 158–162, doi:10.1071/EN11143, 2012.

Snider, D., Thompson, K., Wagner-Riddle, C., Spoelstra, J. and Dunfield, K.: Molecular techniques and stable isotope ratios

445 at natural abundance give complementary inferences about N$_2$O production pathways in an agricultural soil following a rainfall event, Soil Biol. Biochem., 88, 197–213, doi:10.1016/j.soilbio.2015.05.021, 2015.

Snider, D. M., Venkiteswaran, J. J., Schiff, S. L. and Spoelstra, J.: Deciphering the oxygen isotope composition of nitrous oxide produced by nitrification, Glob. Chang. Biol., 18(1), 356–370, doi:10.1111/j.1365-2486.2011.02547.x, 2012.

Snider, D. M., Venkiteswaran, J. J., Schiff, S. L. and Spoelstra, J.: A new mechanistic model of δ^{18}O-N$_2$O formation by

450 denitrification, Geochim. Cosmochim. Acta, 112, 102–115, doi:10.1016/j.gca.2013.03.003, 2013.

Sutka, R. L., Ostrom, N. E., Ostrom, P. H., Gandhi, H. and Breznak, J. A.: Nitrogen isotopomer site preference of N$_2$O produced by Nitrosomonas europaea and Methylococcus capsulatus Bath, Rapid Commun. Mass Spectrom., 17(7), 738–745, doi:10.1002/rcm.968, 2003.

Sutka, R. L., Ostrom, N. E., Ostrom, P. H., Breznak, J. A., Pitt, A. J., Li, F. and Gandhi, H.: Distinguishing nitrous oxide

455 production from nitrification and denitrification on the basis of isotopomer abundances, Appl. Environ. Microbiol., 72(1), 638–644, doi:10.1128/AEM.72.1.638, 2006.

Sutka, R. L., Adams, G. C., Ostrom, N. E. and Ostrom, P. H.: Isotopologue fractionation during N$_2$O production by fungal denitrification, Rapid Commun. Mass Spectrom., 22(24), 3989–3996, doi:10.1002/rcm.3820, 2008.

Tallec, G., Garnier, J., Billen, G. and Gousailles, M.: Nitrous oxide emissions from secondary activated sludge in nitrifying

460 conditions of urban wastewater treatment plants: Effect of oxygenation level, Water Res., 40(15), 2972–2980, doi:10.1016/j.watres.2006.05.037, 2006.

Tanaka, H. and Dunn, I. J.: Kinetics of biofilm nitrification, Biotechnol. Bioeng., 24(3), 669–689, doi:10.1002/bit.260240311, 1982.

Terada, A., Sugawara, S., Hojo, K., Takeuchi, Y., Riya, S., Harper, W. F., Yamamoto, T., Kuroiwa, M., Isobe, K., Katsuyama,

465 C., Suwa, Y., Koba, K. and Hosomi, M.: Hybrid nitrous oxide production from a partial nitrifying bioreactor: hydroxylamine interactions with nitrite, Environ. Sci. Technol., 51(5), 2748–2756, doi:10.1021/acs.est.6b05521, 2017.

Toyoda, S., Suzuki, Y., Hattori, S., Yamada, K., Fujii, A., Yoshida, N., Kouno, R., Murayama, K. and Shiomi, H.: Isotopomer analysis of production and consumption mechanisms of N_2O and CH_4 in an advanced wastewater treatment system, Environ. Sci. Technol., 45(3), 917–922, doi:10.1021/es102985u, 2011.

470 Toyoda, S., Yoshida, N. and Koba, K.: Isotopocule analysis of biologically produced nitrous oxide in various environments, Mass Spectrom. Rev., 36(2), 135–160, doi:10.1002/mas.21459, 2017.

Vieten, B., Blunier, T., Neftel, A., Alewell, C. and Conen, F.: Fractionation factors for stable isotopes of N and O during N_2O reduction in soil depend on reaction rate constant, Rapid Commun. Mass Spectrom., 21(6), 846–850, doi:10.1002/rcm.2915, 2007.

475 Webster, E. A. and Hopkins, D. W.: Nitrogen and oxygen isotope ratios of nitrous oxide emitted from soil and produced by nitrifying and denitrifying bacteria, Biol. Fertil. Soils, 22(4), 326–330, doi:10.1007/BF00334577, 1996.

Wunderlin, P., Mohn, J., Joss, A., Emmenegger, L. and Siegrist, H.: Mechanisms of N_2O production in biological wastewater treatment under nitrifying and denitrifying conditions, Water Res., 46(4), 1027–1037, doi:10.1016/j.watres.2011.11.080, 2012.

Wunderlin, P., Lehmann, M. F., Siegrist, H., Tuzson, B., Joss, A., Emmenegger, L. and Mohn, J.: Isotope signatures of N_2O

480 in a mixed microbial population system: Constraints on N_2O producing pathways in wastewater treatment, Environ. Sci. Technol., 47(3), 1339–1348, doi:10.1021/es303174x, 2013.

Yamagishi, H., Westley, M. B., Popp, B. N., Toyoda, S., Yoshida, N., Watanabe, S., Koba, K. and Yamanaka, Y.: Role of nitrification and denitrification on the nitrous oxide cycle in the eastern tropical North Pacific and Gulf of California, J. Geophys. Res., 112(G2), doi:10.1029/2006JG000227, 2007.

485 Yamazaki, T., Hozuki, T., Arai, K., Toyoda, S., Koba, K., Fujiwara, T. and Yoshida, N.: Isotopomeric characterization of nitrous oxide produced by reaction of enzymes extracted from nitrifying and denitrifying bacteria, Biogeosciences, 11(10), 2679–2689, doi:10.5194/bg-11-2679-2014, 2014.

Yoshida, N.: ^{15}N-depleted N_2O as a product of nitrification, Nature, 335(6190), 528–529, doi:10.1038/335528a0, 1988.

Zhang, L., Altabet, M. A., Wu, T. X. and Hadas, O.: Sensitive measurement of NH_4^+ [15]N/[14]N ($\delta^{15}NH_4^+$) at natural abundance

490 levels in fresh and saltwaters, Anal Chem, 79(14), 5297–5303, doi:Doi 10.1021/Ac070106d, 2007.